We are IntechOpen,
the world's leading publisher of Open Access books
Built by scientists, for scientists

6,900
Open access books available

186,000
International authors and editors

200M
Downloads

Our authors are among the

154
Countries delivered to

TOP 1%
most cited scientists

12.2%
Contributors from top 500 universities

Interested in publishing with us?
Contact book.department@intechopen.com

Numbers displayed above are based on latest data collected.
For more information visit www.intechopen.com

Absorption of Carbon Dioxide in a Bubble-Column Scrubber

Pao-Chi Chen
Graduate School of Engineering Technology
Department of Chemical and Materials Engineering
Lunghwa University of Science and Technology
Taiwan

1. Introduction

In the current stage over 85% of world energy demand is supplied by fossil fuels. Coal-fired plants discharged roughly 40% of the total CO_2 are the main contributors in CO_2 emissions (Kim & Kim, 2004; Yang et al., 2008). Environmental issues caused by exhaust green house gases (GHG) and toxics have become global problems. Through the past studies of five decades, increased GHG levels in atmosphere is believed to cause global warming, in which CO_2 is the largest contributors. International Panel on Climate Change (IPCC) predicts that the CO_2 content in atmosphere may contain up to 570 ppmv CO_2, causing an increase in mean global temperature around 1.9℃ and an increase mean sea level of 38m (Stewart & Hessami, 2005). Also accompanied is species extinction. Therefore, the importance of removing carbon dioxide from exhaust emissions has been recognized around the world. There are three options to reduce total emission into the atmosphere, i. e., to increase energy efficiency, to use renewable energy, and enhance the sequestration or removal of CO_2. However, from the viewpoints of coal-fired plants discharged a lot amount of CO_2-gas, CO_2 gas needs to be removed from the flue gases of such point sources before direct sequestration. There are several processes for CO_2 separation and capture processes, including post-combustion, pre-combustion, oxy-fuel processes, and chemical-looping combustion (Yang et al., 2008). In here, we focus on the treatment of post-combustion processes since they are typical coal-fired plants.

For the removal of exhaust CO_2-gas, several methods have been proposed, such as chemical absorption, physical absorption, membrane separation, biochemical methods, and the catalytic conversion method. In addition to these methods, the absorption of carbon dioxide in an alkaline solution with crystallization has also been adopted to explore the removal of carbon dioxide from waste gas (Chen et al., 2008). This approach, with the production of carbonate by means of reactive crystallization, has been found to be effective. In order to remove of CO_2 gas, several scrubbers were utilized, such as sieve tray column, packed bed column, rotating packed bed and bubble column. Therefore, how to choose an excellent scrubber becomes significant in the removal of CO_2 gas from flue gas. The performances of the scrubbers were always estimated by using overall mass-transfer coefficient. Due to this, they found packed bed with structured packing (Aroonwilas & Tontiwachwuthiku, 1997)

gives a higher overall mass-transfer coefficient as compared with other scrubbers. On the other hand, Chen et al. (2008) found that the performance of scrubber could be estimated by using scrubbing factor, a definition of removal of 1 mole CO_2 gas per mole of absorbent and per liter of scrubber. In this manner, a bubble-column scrubber is the first choice.

In a bubble column, gas is often introduced near the bottom of the column. The liquid may flow through the column either with or against the gas flow. Investigations of bubble-columns from the viewpoints of both environmental problems and industrial use can be found in the literature (Juvekar & Sharma, 1973; Sada et al., 1985; Sauer & Hempel, 1987; Okawa et al., 1999; Chen et al., 2002; Hamid & Jones, 2002; Lapin et al., 2002). Bubble column reactors are widely used in the chemical, petrochemical, biochemical, and metallurgical industries (Degaleesan & Dudukovic, 1998). They were favored because of their simple construction, higher heat and mass transfer coefficients, higher removal efficiency, and effective control of the liquid residence time. In addition, bubble columns may be operated in either batch mode or continuous mode, depending on the requirements, as in processes such as liquid-phase methanol synthesis or continuous-mode Fisher-Tropsch synthesis with a liquid superficial velocity that is lower than the gas superficial velocity by at least an order of magnitude or more. In this manner, the gas flow controls the fluid dynamics of the individual phases of these systems. This in turn controls liquid mixing and inter-phase mass transfer, which subsequently influence conversion and selectivity.

In addition, some investigators (Sauer & Hempel, 1987; Hamid & Jones, 2002) have studied the dynamics, mass transfer, and control of the crystal size and shape of products for industrial purposes. However, these data cannot be utilized effectively. In gas-liquid reaction, the absorption mechanism is controlled by both the mass-transfer and chemical reaction steps, depending on the operating conditions. In order to describe the concentration distributions, several diffusion-with-chemical-reaction models have been proposed in the literature (Sherwood et al., 1975; Shah, 1979; Fan, 1989; Cournil & Herri, 2003). In these reports, the chemical reaction kinetics in gas-liquid reactions was first order or second order, depending on the pH of the solution. However, in some systems the mass action equations were found to be very complicated, and in others, it was found that the pH had an effect on the species (Morel, 1983). Therefore, the absorption of gases was strongly affected by the pH of the solution. Thus, it is clear that controlling the pH of the solution is important for controlling the absorption rates of gases, since the ionic strength and, hence, Henry's constant are affected by the pH of the solution. Additionally, several gas-liquid absorption applications, such as desulfurization processes and the removal of carbon dioxide, involve small particles (Hudson and Rochelle, 1982; Saha and Bandyopadhyay, 1992; Chen et al., 2002; Okawa et al., 1999). However, some of the above papers reported that the size and concentration of solids affected the mass-transfer coefficient, while most studies found larger sizes at higher solid concentrations (Shah, 1979; Cournil & Herri, 2003). These mass-transfer coefficient data cannot be used in absorption with reactive crystallization systems, such as gypsum and carbonates. Therefore, research on the effect of particles on the absorption processes is required. For design purposes, data for the hydrodynamics and mass-transfer coefficients in bubble columns is required (Bukur & Daly, 1987). In order to obtain the mass transfer coefficients in an alkaline solution with and without solids, a two-film model was utilized to describe the absorption of carbon dioxide. The results are also compared here with those reported in the literature.

In this chapter, the materials include absorption models, determination of absorption rate, solution chemistry, determination of mass-transfer coefficients, and scrubbing factors of various scrubbers. Finally, how to estimate the size of bubble-column scrubber is also discussed in this chapter.

2. Absorption models

When gas is blown through the liquid as a stream of bubbles, e. g., in a sparged vessel or on a bubble-plate; diffusion, convection, and reaction proceed simultaneously. A complicated system is formed during gas-liquid contact. Absorption accompanied with chemical reaction not only can enhance the absorption rate but also can reduce the height of scrubber (Levenspiel, 1998). Therefore, in absorption accompanied with chemical reaction system, chemical reaction kinetics play an important role on the overall rate of absorption process. There are eight special cases for the absorption with reaction processes; the absorption efficiency is dependent on fast reaction or slow reaction kinetics. In order to quantitatively evaluate the absorption rate, absorption model proposed is required. Four models are observed in the literature (Danckwerts, 1970; Sherwood et al., 1975); there are the film model, still surface model, surface-renewal model, and the penetration model. In here, a two-film model is introduced, since it is a more practical model for applications, as shown in Figure 1. The gas solute in bulk phase overcomes the resistance of gas film and moves to the gas-liquid interface; later, solute moves across the interface and overcomes the liquid film resistance and goes through the bulk liquid. At the interface the Henry's law is applied:

$$C_i = K_H P_i \tag{1}$$

where C_i is the concentration of solute at liquid side interface, P_i the partial pressure of solute at gas side interface, and K_H the Henry's law constant. The two-film model is widely used in the literature. In here, the Henry's law constant is dependent on the ionic strength and temperature.
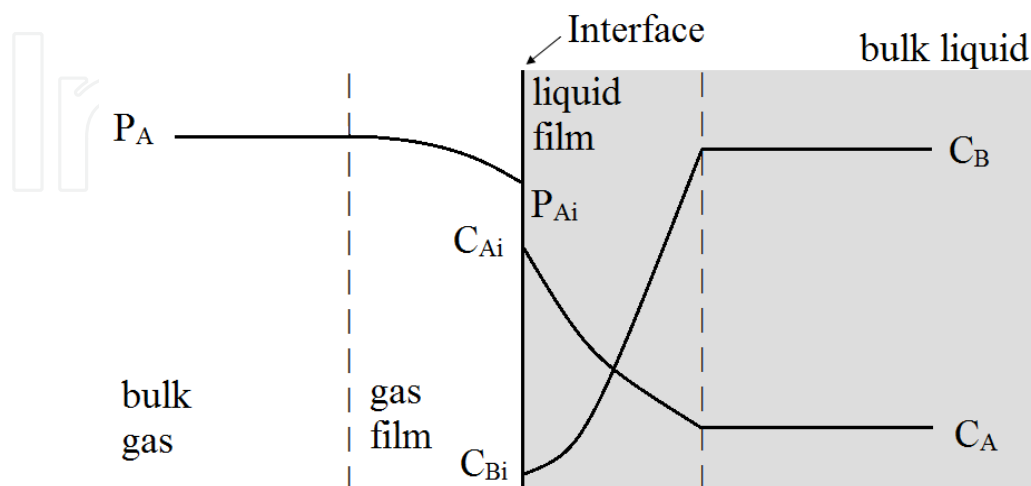

Fig. 1. A schematic diagram for the two-film model.(Levenspiel, 1998)

3. Solution chemistry in carbonate system

When CO_2 dissolves in water, it hydrates to form H_2CO_3. In basic solution, hydrated carbon dioxide ionizes to give hydrated protons $[H^+]$, bicarbonate ion $[HCO_3^-]$, and carbonate ion $[CO_2^{2-}]$. The solution chemistry for CO_2-H_2O system is expressed in terms of Equations (2)-(4). In here, we will abbreviate $[H_2CO_3]+[CO_2]$ simply as $[H_2CO_3^*]$. The total amount of dissolved carbonate increases with increasing pH because of the ionization equilibrium. In dilute solutions at 25℃, the ionization constants for K_{a1} and K_{a2} are approximately $10^{-6.3}$ and $10^{-16.3}$(Butler, 1982), respectively. The ionization constants depend on temperature and on the presence of other salts.

$$CO_2(g) + H_2O = H_2CO_3^* \tag{2}$$

$$H_2CO_3^* = H^+ + HCO_3^- \tag{3}$$

$$HCO_3^- = H^+ + CO_3^{2-} \tag{4}$$

Figure 2 is a plot of degree of ionization (α)versus pH at 25℃. In here, the total amount of carbonate is the summation of all carbons including $H_2CO_3^*$, HCO_3^- and CO_3^{2-}.We express as C_T. In addition, α_0, α_1, andα_2 are the degree of ionization for species $H_2CO_3^*$, HCO_3^- and
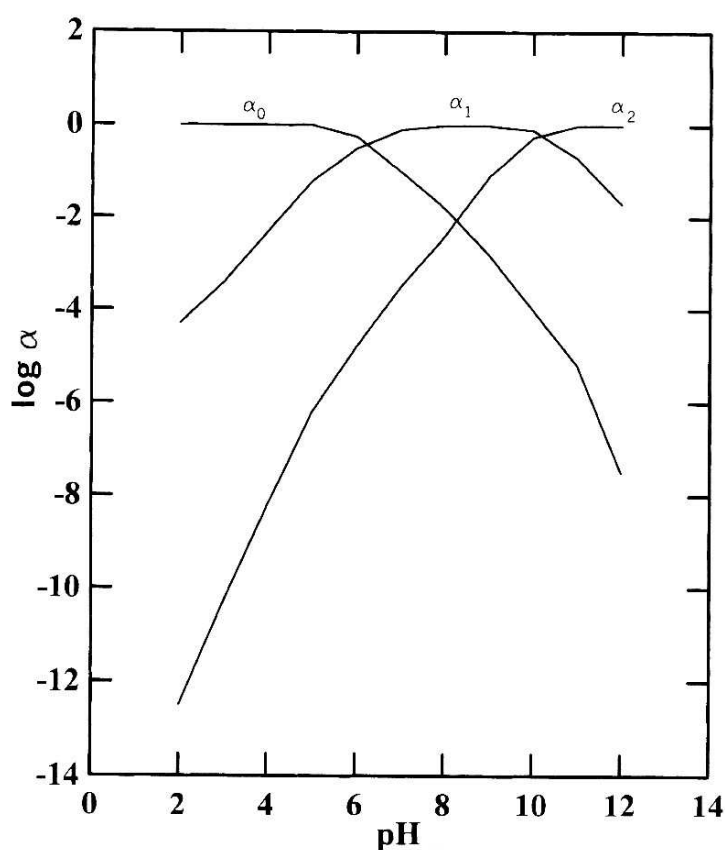
Fig. 2. Ionization of carbon dioxide as a function of pH value $[H_2CO_3^*] = [H_2CO_3] +$ $+[CO_2(aq)]$; $\alpha_0 + \alpha_1 + \alpha_2 = 1$ α_0=$[H_2CO_3^*]$/ C_T; α_1=$[HCO_3^-]$/ C_T; α_2=$[CO_3^{2-}]$/ C_T

$CO_3{}^{2-}$, respectively. It is found that α_0 decreases with an increasing in pH on one hand and α_2 increases with pH on the other hand, while α_1 increases with an increasing in pH when the pH is less than 6 on one hand and it decreases with an increasing with pH when the pH is higher than 10 on the other hand. This indicates that the pH value could be adjusted to desired value to control the chemical species, such as $H_2CO_3{}^*$, $HCO_3{}^-$ and $CO_3{}^{2-}$, presented in the solution. This could be done with an addition of alkaline solution, such as NaOH solution, and acidic solution, such as HCl solution. In order to show the effect of alkaline solution and chemical species on the concentrations of $H_2CO_3{}^*$, $HCO_3{}^-$ and $CO_3{}^{2-}$, an example will be discussed later.

For the CO_2-H_2O-$BaCl_2$ system with an addition of NaOH solution, there are a lot of chemical species presented in the solution, such as $H_2CO_3{}^*$, $HCO_3{}^-$, $CO_3{}^{2-}$, H^+, OH^-, Ba^{2+}, Cl^-, Na^+, and ion pair $BaCO_3{}^0$. Due to this, the mass action equations, total mass balance equations and charge balance equation are shown in Table 1, Eqs. (5)-(15).

Mass action equations: (Morel, 1983)

$$H_2O = OH^- + H^+ \tag{5}$$

$$CO_2(g) + H_2O = H_2CO_3{}^* \tag{6}$$

$$H_2CO_3{}^* = HCO_3^- + H^+ \tag{7}$$

$$HCO_3^- = CO_3^{2-} + H^+ \tag{8}$$

$$BaCO_3^o = Ba^{2+} + CO_3^{2-} \tag{9}$$

$$BaCO_3(s) = Ba^{2+} + CO_3^{2-} \tag{10}$$

Total mass balance equations:

$$TCO = [H_2CO_3{}^*] + [HCO_3^-] + [CO_3^{2-}] + [BaCO_3{}^0] \tag{11}$$

$$TBa = [Ba^{2+}] + [BaCO_3^o] \tag{12}$$

$$TCl = [Cl^-] \tag{13}$$

$$TNa = [Na^+] \tag{14}$$

Charge balance equation

$$[H^+] + 4[Ba^{2+}] + [Na^+] = [OH^-] + [Cl^-] + [HCO_3^-] + 4[CO_3^{2-}] \tag{15}$$

Table 1. Mass action, total mass balance, and charge balance equations.

From a given pH value and the total mass balance equations, mass action equations, and activity coefficient equations, the concentrations of chemical species can be obtained by using an ionic strength approximation method (Butler, 1964; Nancollas, 1966; Chen et al., 2004). Due to this, the ionic strength can be determined. The activity coefficients of electrolytes can be estimated from the Bromley correlation equation (Sohnel & Garside, 1992):

$$\frac{1}{z_i^2}\log\gamma_i = -0.511\frac{\sqrt{I}}{1+\sqrt{I}} + \frac{(0.06+0.6B_1)I}{(1+1.5I/z_i)^2} + \frac{B_1 I}{z_i^2} \tag{16}$$

where z_i is the charge number, I is the ionic strength and B_1 is composed of ionic contributions. This equation can be used to estimate activity coefficients in solutions of high ionic strength up to about 6 M. The ionic strength of a solution can be calculated with the following equation:

$$I = \frac{1}{2}\sum z_i^2 C_i$$
$$= \frac{1}{2}\left([H^+] + 4[Ba^{2+}] + [Na^+] + [OH^-] + [HCO_3^-] + 4[CO_3^{2-}] + [Cl^-]\right) \tag{17}$$

For a bubble column, total chloride ion concentration (*TCl*) and total sodium ion concentration (*TNa*) can be determined from material balances, since chloride and sodium ions are both non-reacting components. At steady-state condition, the *TCl* and *TNa* can be evaluated as follows:

$$TCl = \frac{2Q_1 C_1}{Q_1 + Q_2} \tag{18}$$

and

$$TNa = \frac{Q_2 C_2}{Q_1 + Q_2} \tag{19}$$

where Q_1 and Q_2 are volumetric flow rates for barium chloride solution and sodium hydroxide solution, respectively, C_1 the feed concentration of chloride ion, and C_2 the feed concentration of sodium ion.

Once the ionic strength is obtained, the Henry's law constant, defined in Equation (1), can be evaluated (Butler, 1982). For example, at a temperature of 30℃, Henry's law constant can be expressed as:

$$pK_H = 1.53 + 0.1039I - 0.0148I^2 \tag{20}$$

Where pK_H is defined as:

$$pK_H = -\log K_H \tag{21}$$

Sometime, Henry's law constant is defined as:

$$H = \frac{1}{K_H RT} \tag{22}$$

The Henry's law constant, H, will be used in later.

4. Determination of absorption rate at steady-state

In a bubble column, for a simulated flue gas ($CO_2(N_2)$-H_2O system), as shown in Figure 3, a gas mixture containing A (carbon dioxide) and B (nitrogen) flowing into a bubble column at the bottom comes into continuous contact with an alkaline solution flowing into the column

at the top. Two streams come into contact with in the column adversely. If we assume that nitrogen gas is essentially insoluble in the liquid phase and that liquid does not vaporize to the gas phase, the gas phase is a binary A-B. The absorption rate of carbon dioxide can be determined by using the material balance under steady state operation, as shown in Figure 3 for a multiple-tube plug-flow model. If we assume plug flow for the gas phase through the tube, the material balance for carbon dioxide in the ith tube at steady state is

$$(u_i C_{Ai}\big|_z - u_i C_{Ai}\big|_{z+\Delta z})S_i - r_{Ai}\pi d_i \Delta z = 0 \tag{23}$$

where u_i is the linear velocity, S_i the cross section of ith tube, r_{Ai} the absorption rate per unit area of the ith tube, and d_i the diameter of ith tube. For a total of N tubes the material balance becomes

$$\sum_{i=1}^{N} S_i(u_i C_{Ai}\big|_z - u_i C_{Ai}\big|_{z+\Delta z}) - \sum_{i=1}^{N} r_{Ai}\pi d_i \Delta z = 0 \tag{24}$$

Equation (24) divided by Δz and taken to the limit, $i.e.$, $\Delta z \to 0$, Equation (24) becomes

$$-\frac{d(\sum u_i S_i C_{Ai})}{dz} - \sum_{i=1}^{N} r_{Ai}(\pi d_i) = 0 \tag{25}$$

or

$$-\frac{dF_A}{dz} - \sum_{i=1}^{N} r_{Ai}(\pi d_i) = 0 \tag{26}$$

where F_A is the overall molar flow rate of the gas phase, which is equal to $\sum u_i S_i C_{Ai}$. Integrating Equation (26), we have

$$-\int_1^2 dF_A - \sum_{i=1}^{N} \int_1^2 r_{Ai}(\pi d_i)dz = 0 \tag{27}$$

and

$$(F_{A1} - F_{A2}) - \int_1^2 \sum_{i=1}^{N} r_{Ai}dA_i = 0 \tag{28}$$

where A_i is the lateral surface area of the ith tube. These equations can be rewritten as

$$(F_{A1} - F_{A2}) - \overline{r}_A A = 0 . \tag{29}$$

and

$$\overline{r}_A = \frac{\sum\int_1^2 r_{Ai}dA_i}{\sum\int_1^2 dA_i} = \frac{\sum\int_1^2 r_{Ai}dA_i}{A} \tag{30}$$
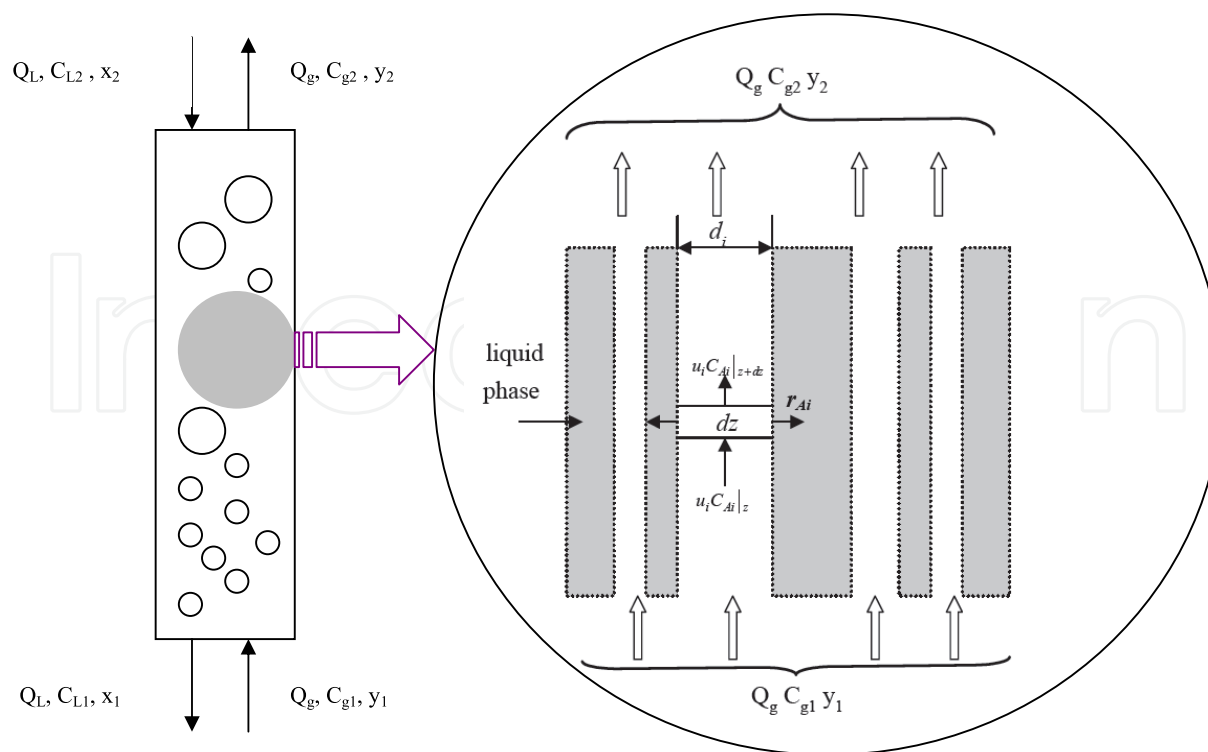
Fig. 3. A multiple-tube plug flow model.

where $\overline{r}_A$ is the mean absorption rate and A is the total surface area of the gas phase in the bubble column, which can not be obtained directly. Equation (29) shows that the absorption rate, $\overline{r}_A A$, is equal to the consumption of carbon dioxide through the bubble column. This value can be determined by measuring the concentration of carbon dioxide and the gas-flow rate:

$$R_A = \frac{F_{A1} - F_{A2}}{V_L} = \frac{F_{A1} - F_{A2}}{\varepsilon_L V_b} \tag{31}$$

and

$$R_A = \frac{\overline{r}_A A}{V_L} \tag{32}$$

where V_L is the volume of the liquid phase, V_b the volume of the bubble column, and ε_L is the hold-up of the liquid phase. Since the molar flow rate of inert gas is equal to $F_{A1}(1-y_1)/y_1$, the molar flow rate of acidic gas at the outlet, F_{A2}, is $F_{A1}[(1-y_1)/y_1][y_2/(1-y_2)]$. Thus, Equation (31) can be rewritten as

$$R_A = \frac{F_{A1}}{V_L}\left[1 - (\frac{1-y_1}{y_1})(\frac{y_2}{1-y_2})\right] \tag{33}$$

Therefore, the overall absorption rate, R_A, as defined by Cournil & Herri (2003), can be obtained with measurable quantities. Figure 4 exhibits the absorption rate versus gas-flow rate with precipitation at various pH values. The result shows that the absorption rate

increased with an increase in gas-flow rate as well as pH value. In addition, the absorption rate also increased obviously with an increase in gas concentration, y_1, but was only slightly affected by liquid-flow rate.
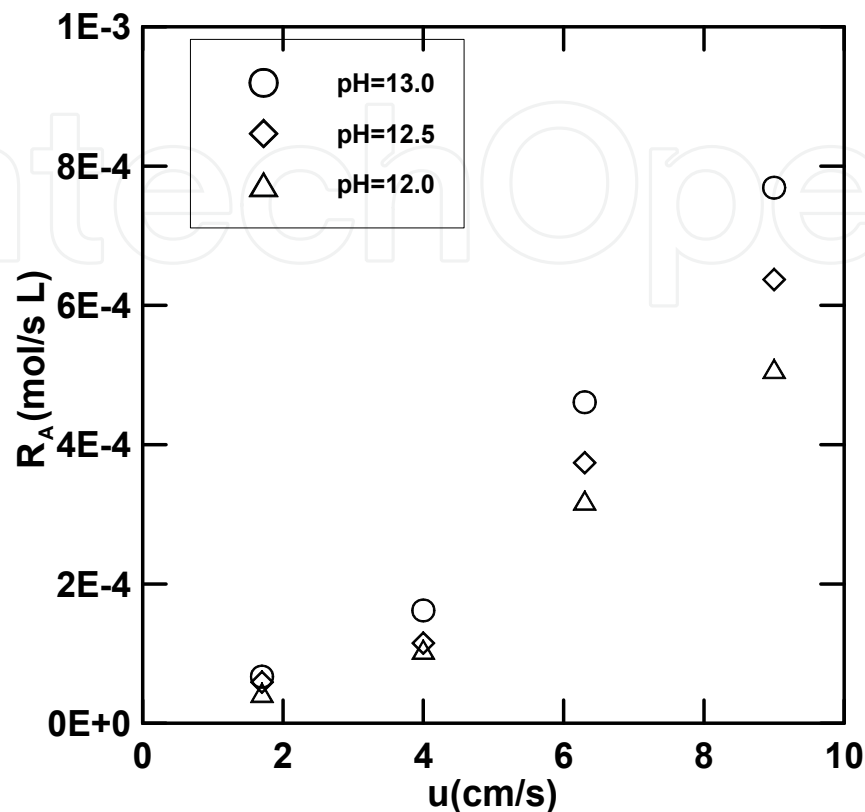

Fig. 4. A plot of R_A versus u at various pH values.

5. Determination of mass-transfer coefficients

According to a two-film model for $CO_2(N_2)$-H_2O system, the relationship between local absorption rate, r_A, and local individual mass-transfer coefficients based on both the gas-side and liquid-side can be written as

$$r_A = k_G a(C_g - C_{gi}) \tag{34}$$

$$= k_L a(C_{Li} - C_L) \tag{35}$$

at the interface $C_{gi} = HC_{Li}$, where H is Henry's law constant defined in Equation (2). Combining Equation (34) and Equation (35) in terms of the overall mass-transfer coefficient, the equation becomes

$$r_A = (K_G a)_{loc}(C_A - HC_{LA}) \tag{36}$$

where, C_A and C_{LA} are concentrations of CO_2-gas in the gas-phase and liquid-phase, respectively. According to Equation (24), we assume plug flow for gas phase and well-mixed flow for liquid phase, the material balance equation between Δz at steady state can be rewritten as:

$$(uC_A\big|_z - uC_A\big|_{z+\Delta z})S - r_A \varepsilon_L S \Delta z = 0 \tag{37}$$

Where, u is the mean gas-superficial velocity based on the column cross-sectional area. Take limit for Equation (37),

$$u\frac{dC_A}{dz} + r_A \varepsilon_L = 0 \tag{38}$$

Substitute Equation (36) into Equation (38),

$$u\frac{dC_A}{dz} + (K_G a)_{loc}(C_A - HC_{AL})\varepsilon_L = 0 \tag{39}$$

In Equation (39), C_{AL} is almost less than 4×10^{-8} M when the pH value is higher than 12. In addition, H value is around 1.5 and C_A is higher than 1mM. Therefore, $C_A >> HC_{LA}$, Equation (39) could be written as

$$u\frac{dC_A}{dz} + (K_G a)_{loc} C_A \varepsilon_L = 0 \tag{40}$$

We assume that ε_L is kept constant through the column. Integrating Equation (40), we have

$$u\int_{C_{A1}}^{C_{A2}} \frac{dC_A}{C_A} + \varepsilon_L \int_0^L (K_G a)_{loc}\, dz = 0 \tag{41}$$

and,

$$u\ln\frac{C_{A2}}{C_{A1}} + K_G a L \varepsilon_L = 0 \tag{42}$$

where,

$$K_G a = \frac{1}{L}\int_0^L (K_G a)_{loc}\, dz \tag{43}$$

By multiplying S with Equation (42), the equation becomes

$$K_G a = \frac{Q_g}{V_L}\ln\frac{C_{A1}}{C_{A2}} \tag{44}$$

Using this equation, the average overall mass-transfer coefficient can be evaluated in terms of measurable quantities.

Furthermore, the overall mass-transfer coefficient is correlated with the individual mass-transfer coefficients:

$$\frac{1}{K_G a} = \frac{1}{k_G a} + \frac{H}{k_L a} \tag{45}$$

Here, $1/K_Ga$ was overall resistance, $1/k_Ga$ the gas-side resistance, and H/k_La the liquid-side resistance. For a second order reaction, by introducing the enhancement factor into Equation (45), we have

$$\frac{1}{K_Ga} = \frac{1}{k_Ga} + \frac{1}{((D_Ak_2)^{1/2}a)}\frac{H}{C_{B0}^{1/2}},$$ (46)

where k_2 is the second order reaction constant and D_A is the diffusion coefficient for carbon dioxide. Since Henry's constant is a function of the ionic strength and temperature, which can be adjusted with pH values and temperature, a plot of Equation (46) to obtain k_Ga and k_La becomes possible.

5.1 Comparisons of absorption rates overall mass-transfer coefficients

In here, we will compare absorption rate and overall mass transfer coefficient obtained in a bubble-column scrubber for five absorption systems, i.e., $NaOH/BaCl_2/H_2O$, $NaOH/Zn(NO_3)_2/H_2O$, $MEA/CO_2/H_2O$, $MEA/CaCl_2/CO_2$, and $NH_3/CO_2/H_2O$. The process variables are working temperature, gas-flow rate, pH value, and gas concentration. The absorption rates and overall mass transfer coefficients are listed in Table 2. The table shows that the absorption rates obtained for $NaOH/Zn(NO_3)_2/H_2O$ system were in the range of 1.34×10^{-4}-2.88×10^{-3}mol/L.s, which were higher than that the other systems. However, the absorption rates for $NH_3/CO_2/H_2O$ system were in the range of 2.17×10^{-4}-1.09×10^{-3} mol/L.s; the values were comparable with that $NaOH/Zn(NO_3)_2/H_2O$ system. On the other hand, the overall mass-transfer coefficients obtained for $MEA/CO_2/H_2O$ system were higher than the others, while the values for $NH_3/CO_2/H_2O$ and $NaOH/Zn(NO_3)_2/H_2O$ systems were also comparable with the $MEA/CO_2/H_2O$ system. By means of Taguchi's analysis for $MEA/CO_2/H_2O$ system, the significance sequence influencing the absorption rate is $A(CO_2\%) > C(\text{temperature}) > D(\text{gas-flow rate}) > B(\text{pH})$, while the significance sequence for mass-transfer coefficient is $B > A > C > D$.

5.2 Individual mass-transfer coefficients

A plot of $1/K_Ga$ vs. $H/(C_{B0})^{1/2}$ at different gas-superficial velocity was shown in Figure 5. A linear plot was obtained in this work. The reciprocal of the intercept at zero $H/(C_{B0})^{1/2}$ was the individual gas-side volumetric mass transfer coefficient. On the other hand, the slope, $1/((D_Ak_2)^{1/2}a)$, multiplied by $H/C_{B0}^{1/2}$ was H/k_La, where the liquid-side mass transfer k_La could be obtained.

Figure 6 is a plot of the liquid-side mass transfer coefficient vs. the gas-superficial velocity at various pH values for both with and without precipitation. The liquid-side mass transfer coefficient increased with an increase in the superficial velocity at various pH values. Both procedures show that the data are close together, larger data points for precipitation and smaller data points for no precipitation. The values obtained in this study were higher than those reported by Fan (1989), as shown in the parallelogram, while the values were close to the values reported by Sada et al. (1985). On the other hand, the trend in our data, extrapolated into smaller gas-superficial velocity, was higher than that reported in Sanchez et al. (2005). A linear regression for k_La /$[OH^-]^{0.5}$ and u was found to be:

Systems	Operating conditions	R_A (mol/L · s)	$K_Ga(1/s)$
MEA/CO_2/H_2O	T=25 - 45℃ y_1=15% Q_g=4 - 9.5 L/min C_{MEA}=4 M	$1.35 \times 10^{-6} - 6.22 \times 10^{-4}$	$0.027 - 1.120$
MEA/$CaCl_2$/CO_2 (with precipitation)	T=25℃ y_1=10 - 30% pH=9 - 11 C_L=0.2 M C_{MEA}=4 M Q_g =2L/min- 9.5L/min	$6.26 \times 10^{-6} - 3.69 \times 10^{-4}$	0.018-0.249
NH_3/CO_2/H_2O (with precipitation)	T=25 - 60℃ y_1=15 - 60% pH=9.5 - 11.5 C_{NH3}=7.7 M Q_g=2 - 5 L/min	$2.17 \times 10^{-4} - 1.09 \times 10^{-3}$	$0.0136 - 0.567$
NaOH/$BaCl_2$/H_2O (with precipitation)	T=25℃ y_1=10 - 30% pH=12 - 13 C_L=0.01-0.2 M C_{NaOH}=1-2 M Q_L=50 - 320 ml/min Q_g=2 - 10.7 L/min	$4.4 \times 10^{-5} - 7.69 \times 10^{-4}$	$0.0277 - 0.196$
NaOH/$BaCl_2$/H_2O (without precipitation)	T=25℃ y_1=20% pH=12 - 13 C_{NaOH}=1-2 M Q_L=50 ml/min Q_g=2 – 10.7 L/min	$1.03 \times 10^{-4} - 1.13 \times 10^{-3}$	$0.0651 - 0.339$
NaOH/$Zn(NO_3)_2$/H_2O (with precipitation)	T=25 - 45℃ y_1=20% pH=10 -13 C_L=0.2 M C_{NaOH}=2 M Q_L=50 ml/min Q_g=3 - 8 L/min	$1.34 \times 10^{-4} - 2.88 \times 10^{-3}$	$0.0145 - 0.590$

Table 2. Absorption rates and overall mass-transfer coefficients in a bubble-column scrubber for different systems.
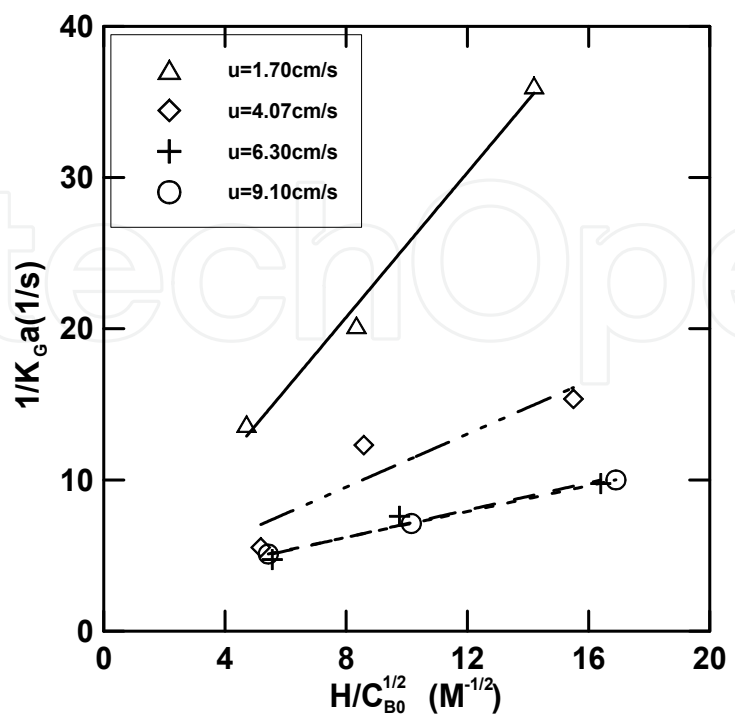
Fig. 5. A plot of $1/K_Ga$ versus $H/C_{B0}^{1/2}$ for obtaining individual mass transfer coefficients (Chen et al., 2008)
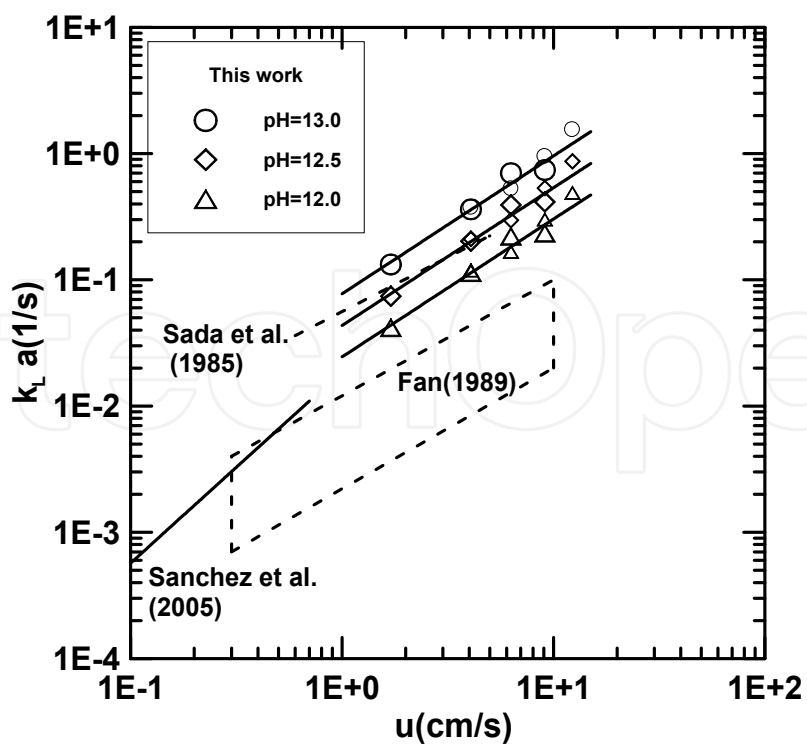

Fig. 6. Effects of process variables on the liquid side mass transfer coefficient.(Chen et al., 2008)

$$k_L a = 0.2449 u^{1.09} [OH^-]^{0.5} \qquad (47)$$

The coefficient of determination becomes 0.9670. The exponent of u in here was 1.09, which falls in the exponent range of 0.58 to 1.52 reported in the literature. In the same absorption system, a correlation for gas-side mass transfer coefficient obtained by using regression for no precipitation system was shown below:

$$k_G a = 0.29982 u^{0.22} \qquad (48)$$

The exponent of u in here was 0.22, which is lower than 0.75 reported in the literature (Sada et al., 1985; Botton et al., 1980). Due to this, the individual mass-transfer coefficients, $k_L a$ and $k_G a$, could be determined when the operating conditions were given; and hence, the overall mass-transfer coefficient was estimated by Equation (45).

6. Scrubbing factor

The scrubbing factor (φ) was defined as $\varphi = (F_g E / F_A V_b)$, which means moles of CO_2-gas to be removed per mole of absorbent and per the volume of the scrubber, estimated values for various scrubbers were also calculated and listed in Table 3. In these systems, F_A is defined as the molar flow rate of absorbent solution. The result showed that φ values in here, both for systems with precipitation and without precipitation, are much higher than those in packed bed systems, indicating that bubble-column scrubbers are indeed more effective than packed bed scrubbers. The scrubbing factors for bubble columns are approximation 5-fold to 20-fold as compared with packed beds. This indicates that the absorption capacity for bubble columns is higher than that for packed beds. Alternatively, comparison for various bubble columns, i.e., $NaOH/BaCl_2/H_2O$ system (1), $NaOH/Zn(NO_3)_2/H_2O$ system(2), $NH_3/CO_2/H_2O$ system(3), and $MEA/CO_2/H_2O$ system(4), is carried out in here, we find that the magnitude sequence in scrubbing factors are (1)>(3)>(4)>(2). In the current stage system (4) is a more popular system in the removal of carbon dioxide. However, system (3) is a more attractive process since aqueous ammonia absorbent has a lot of advantages, including higher absorption capacity, cheaper, lower energy required from the viewpoint of regeneration, no corrosion problem, and safety, as compared with MEA process (Yeh & Bai, 1999; Yeh et al., 2005). Ammonia scrubbing process is widely applied to produce ammonia bicarbonate (ABC) as a fertilizer in the Chinese chemical industry.

Scrubbers	Operating conditions	$K_G a$(1/s)	$\varphi = (F_g E / F_A V_b)$ (mol/mol-L)
Packed bed (Tontiwachwuthiku et al., 1992)	Q_g=0.87-1.47L/min Q_L=1230-1760ml/min y_1=11.5-19.5% [NaOH]=1.2-2.0M	-	1.33×10^{-3}-6.56×10^{-3}
Packed bed (Aroonwilas and Tontiwachwuthiku,1997)	-	0.08-0.27*	-
Packed bed with structured packing (Aroonwilas and Tontiwachwuthiku,1997)	Q_g=4.9-10.4L/min Q_L=23-70ml/min y_1=1-15% [NaOH]=1.0-2.0M	0.68-2.74*	0.0176-0.173

	Q_g=4.9-10.4L/min Q_L=46mL/min AMP=1.1M	0.07	-
RPB (Lin et al, 2003)	Q_g=4.4-13.1L/min Q_L=42ml/min y_1=1-10% [NaOH]=2.0M	0.41-0.53**	0.0508-0.151***
	Q_g=4.4-13.1L/min Q_L=42mL/min AMP=1.0M	0.14	-
	Q_g=4.4-13.1L/min Q_L=42mL/min [MEA]=2.0M [MEA+AMP]=2M	0.50-0.75 0.41-0.51	-
Bubble column without precipitation $NaOH/BaCO_3/H_2O$ (Chen et al., 2008)	Q_g=4.7-14.5 L/min Q_L=50ml/min y_1=20% [NaOH]= 2.0M T=25℃ pH=9.0-12.0	0.0651-0.3396	0.178-0.872
Bubble column with precipitation $NaOH/BaCl_2/H_2O$ (Chen et al., 2008)	Q_g=2.0-10.27 L/min Q_L=50-320ml/min C_L=0.01-0.2M y_1=10-30% [NaOH]= 2.0M	0.0227-0.2115	0.0422-0.637
Bubble column without precipitation $MEA/H_2O/CO_2$ (Chen et al., 2010)	Q_g=4.0-9.5 L/min Q_L=31.35-215.13ml/min y_1=15-65% [MEA]= 4.0M T=25-45℃ pH=9.0-11.0	0.027-1.1204	0.118-0.494
Bubble column (with precipitation) $NH_3/CO_2/H_2O$ (Chen et al., 2010)	T=25 - 60℃ y_1=15 - 60% pH=9.5 - 11.5 C_{NH3}=7.7 M Q_g=2 - 5 L/min	0.0136－0.5669	0.0251-0.664
Bubble column (with precipitation) $NaOH/Zn(NO_3)_2/H_2O$ (Chen et al., 2010)	T=25 - 45℃ y_1=20% pH=10 -13 C_L=0.2 M C_{NaOH}=2 M Q_L=50 ml/min Q_g=3 - 8 L/min	0.0145－0.590	0.0275-0.401

∗:'a' is based on volume of packing;∗∗: 'a' is based on dispersion phase; ∗∗∗: E is assumed to be 0.8.

Table 3. Scrubbing factors for different absorption systems

7. Sizes of bubble-column scrubbers

For a second order instantaneous chemical reaction system, Equation (39) can be applied for gas-side material balance:

$$u\frac{dC_A}{dz} + (K_G a)_{loc}(C_A - HC_{AL})\varepsilon_L = 0 \tag{39}$$

Integrating equation (39) from 0 to Z, we have

$$u\int_{C_{A1}}^{C_{A2}} \frac{dC_A}{C_A - HC_{AL}} + \varepsilon_L K_G a Z = 0 \tag{49}$$

where

$$K_G a = \frac{1}{Z}\int_0^Z (K_G a)_{loc}\, dz \tag{50}$$

Combination of overall mass-transfer coefficient, Equation (49) becomes

$$Z = \frac{u}{\varepsilon_L K_G a}\int_{C_{A2}}^{C_{A1}} \frac{dC_A}{C_A - HC_{AL}} = \frac{u}{\dfrac{\varepsilon_L}{\dfrac{1}{k_G a} + \dfrac{H}{k_L a}}}\int_{C_{A2}}^{C_{A1}} \frac{dC_A}{C_A - HC_{AL}} \tag{51}$$

or

$$V_b = \frac{F_{A1}}{C_{A1}\varepsilon_L K_G a}\int_{C_{A2}}^{C_{A1}} \frac{dC_A}{C_A - HC_{AL}} = \frac{F_{A1}}{\dfrac{C_{A1}\varepsilon_L}{\dfrac{1}{k_G a} + \dfrac{H}{k_L a}}}\int_{C_{A2}}^{C_{A1}} \frac{dC_A}{C_A - HC_{AL}} \tag{52}$$

where $V_b(=SZ)$ is the volume of scrubber and F_{A1} is the molar flow rate of input gas. If $C_A >> HC_{LA}$, Equation (52) could be written as:

$$V_b = \frac{F_{A1}}{C_{A1}\varepsilon_L K_G a}\ln\frac{C_{A1}}{C_{A2}} = \frac{F_{A1}}{\dfrac{C_{A1}\varepsilon_L}{\dfrac{1}{k_G a} + \dfrac{H}{k_L a}}}\ln\frac{C_{A1}}{C_{A2}} \tag{53}$$

Equation (53) shows that the size of scrubber is dependent on gas-flow rate, H (ionic strength and temperature), the pH of the solution, liquid hold-up (ε_L), and desired CO_2 output concentration (C_{A2}). In here, $k_G a$ and $k_L a$ can be evaluated by using Equations (47) and (48) if pH and u are given. In addition, liquid hold-up (ε_L) can be estimated according to Figure 7, a plot of 1-ε_L(gas hold-up) versus $u(\dfrac{1}{\rho}\times\dfrac{72}{\sigma})^{1/3}$, where ρ and σ are the density and surface tension of the liquid in cgs unit. The final correlation has been given as a curve on

log-log coordinates, which can be represented well by the following Equation (Hikita et al., 1980):

$$1 - \varepsilon_L = \frac{1}{2 + (0.35 / u)[(\rho / 1)(\sigma / 72)]^{1/3}} \tag{54}$$

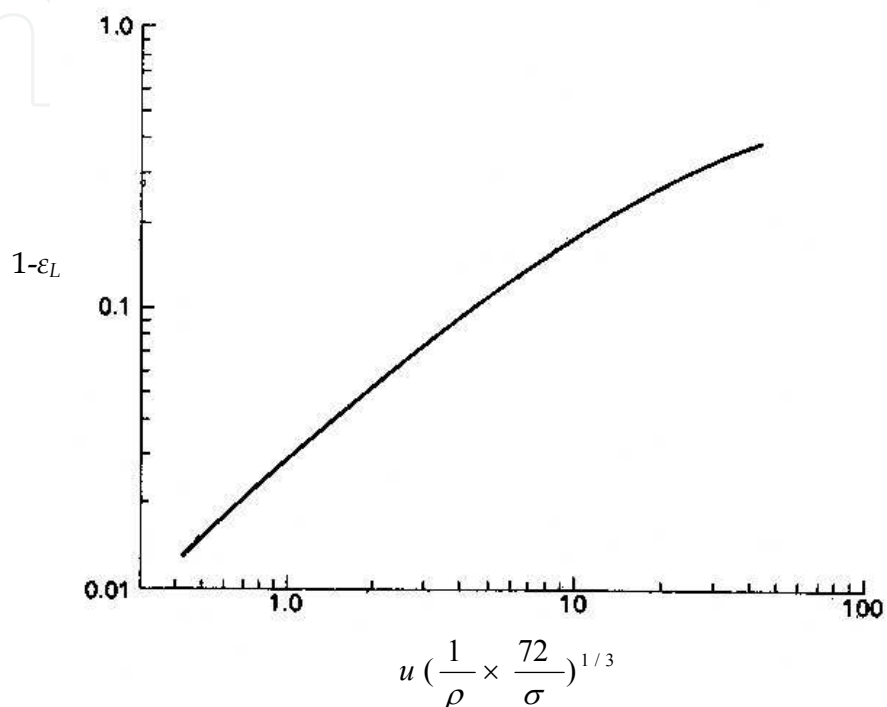Some useful correlations for gas hold-up can be found in the literature (Hikita et al., 1980).

Fig. 7. Gas hold-up in bubble-columns (Danckwerts, 1970)

On the other hand, H can be calculated by using Equations (20) and (22) when the ionic strength and temperature are given. Sometime if overall mass-transfer coefficient correlation is obtained, such as MEA/CaCl$_2$/CO$_2$ with precipitation system, the overall mass-transfer coefficient can be estimated when u and pH of the solution are available:

$$K_G a = 2.62 \times 10^{-5} u^{1.76} \exp(0.41 pH) \tag{55}$$

8. Conclusion

In this chapter, absorption of CO$_2$ in a continuous bubble-column scrubber was illustrated for four absorption systems. In order to obtain absorption rate and mass-transfer coefficients in an alkaline solution with and without precipitation, a two-film model with fast reaction case was utilized to study the absorption of carbon dioxide. A multiple-tube plug flow model was developed to determine the absorption rate and overall mass-transfer coefficient. At the gas-liquid interface, the Henry's law is applied to connect between the bulk phases. In order to determine Henry's law constant, the ionic strength can be determined by using an ionic strength approximation method, if the pH of solution, the total mass balance equations, mass action equations, and activity coefficient equations are available.

Combinations of mass-transfer rate, overall mass-transfer coefficient, Henry's law constant and individual mass-transfer coefficients, the overall mass-transfer coefficient can correlate with the individual mass-transfer coefficients. For a second order reaction, by introducing the enhancement factor into correlation equation, we can obtain both gas-side and liquid-side individual mass-transfer coefficients by using measurable data. The effects of process variables on the individual mass-transfer coefficients were discussed and we obtained kinetic expressions for the both. Using Taguchi's analysis for $MEA/H_2O/CO_2$ system, it was found that the significance sequence influencing the absorption rate is $A(CO_2\%) > C(temperature) > D(gas-flow\ rate) > B(pH)$, while the significance sequence for mass-transfer coefficient is $B > A > C > D$. According to scrubbing factor defined in here, it was found that the scrubbing factors for bubble columns are always higher than that packed beds. This illustrates a higher scrubbing capacity for bubble columns as compared with packed beds. Finally, according to the material balance model proposed in here, the size of bubble column scrubber could be evaluated when the individual mass-transfer coefficients are available.

9. Acknowledgement

10. Nomenclature

A= total surface area of bubbles in scrubber (cm²)

a= gas-liquid interfacial area based on the slurry volume (1/cm)

B_1= a constant in Eq.(16)

C_A= concentration of component A (mol/L)

C_B= concentration of component B (mol/L)

C_{A1}= concentration of A in gas phase at inlet (mol/L)

C_{A2}= concentration of A in gas phase at outlet (mol/L)

C_{Ai}= concentration of A at gas side interface (mol/L)

C_{Bi}= concentration of B at liquid side interface (mol/L)

C_1= concentration of chloride ion at the inlet (mol/L)

C_2= concentration of NaOH at the inlet (mol/L)

C_{B0}= concentration of hydroxide ion (mol/L)

C_g=concentration of solute in bulk gas phase (mol/L)

C_{g1}=concentration of CO_2-gas at inlet (mol/L)

C_{g2}=concentration of CO_2-gas at outlet (mol/L)

C_L= concentration of solute in solution (mol/L)

C_{LA}= concentration of component A in liquid phase (mol/L)

C_T=total carbonate concentration (mol/L)

D_A= diffusivity (cm^2/s)

E= removal efficiency

F_{A1}= molar flow rate of the CO_2-gas at the inlet (mol/s)

F_{A2}=molar flow rate of the CO_2-gas at the outlet (mol/s)

F_g= gas-molar-flow rate (mol/s)

F_L= liquid-molar-flow rate (mol/s)

F_A= absorbent A molar-flow rate (mol/s)

H= Henry's law constant

I= ionic strength (mol/L)

k_2= second order reaction constant (L/mol s)

$k_L a$= individual volumetric liquid-side mass-transfer coefficient (s^{-1})

$k_G a$= individual volumetric gas-side mass-transfer coefficient (s^{-1})

$K_G a$= overall mass-transfer coefficient (s^{-1})

$(K_G a)_{loc}$= local mass-transfer coefficient (s^{-1})

K_H= Henry's constant defined in Eq.(1)

L=height of the bubble column (cm)

P_i= partial pressure of component i (atm)

P_{Ai}= partial pressure of component A at interface (atm)

Q_1=feed rate of $BaCl_2$ solution (mL/min)

Q_2=feed rate of NaOH solution (mL/min)

Q_g= gas-flow rate (L/min)

Q_L= feed rate of liquid solution (mL/min)

R= universal gas constant (atm-L/K mol)

R_A=absorption rate (mol/s L)

r_A=mass-transfer rate (mol/s cm^2)

$\overline{r_A}$ =average mass-transfer rate defined in Eq.(30)(mol/s cm^2)

S=cross section area (cm^2)

T= absolute temperature (K)

TBa= total barium ion concentration (mol/L)

TCO= total carbonate ion concentration (mol/L)

TCl= total chloride ion concentration (mol/L)

TNa= total sodium ion concentration, mol/L

u= superficial velocity (cm/s)

V_b= volume of the bubble column (L)

V_L= volume of liquid in bubble column (L)

y_1=molar fraction of CO_2-gas at the inlet (%)

y_2=molar fraction of CO_2-gas at the outlet (%)

z= position in the bubble column (cm)

Greek symbols

α_i=degree of ionization, i=0,1,2

γ_i= activity coefficient

ε_L= hold-up of liquid

ρ=density of fluid (g/cm^3)

σ=surface tension (dyn/cm)

φ= scrubbing factor (mol-CO_2/mol·L)

11. References

Aroonwilas, A.; Tontiwachwuthikul, P. (1997). High-efficiency Structured Packing for CO_2 Separation Using 2-amino-2-methyl-1-propanol(AMP). *Separation and Purification Technology*, *12*, pp.67-79.

Botton, R., Cosserrat, D. and Charpentier, J. C. (1980). Mass Transfer in Bubble Columns Operating at High Gas Throughputs, *Chem. Eng. J.*, 20, pp.87-94.

Butler, J. N. (1964). *Ionic Equilibrium*, Addison-Wesley Publishing Company, Inc., USA.

Butler, J. N. (1982). *Carbon Dioxide Equilibriua and Their Applications*, Addison-Wesley Publishing Company, Inc., USA.

Bukur, D. B. and Daly, J. G. (1987). Gas hold-up in bubble columns for Fischer-Tropsch synthesis, *Chem. Eng. Sci.*, 42(12), pp.2967-2969.

Chen, P. C.; Shi, W.; Du, R.; Chen, V. (2008). Scrubbing of CO_2 greenhouse gas accompanying with precipitation in a continuous bubble-column scrubber, *I&EC* , 47, pp.6336-6343.

Chen, P. C.; Chen, C. C.; Fun, M. H.; Liao, O. Y.; Jiang, J. J.; Wang, Y. S.; Chen, C. S. (2004). Mixing and Crystallization Kinetics in Gas-liquid Reactive Crystallization. *Chem. Eng. Tech.*, *27*, pp.519-531.

Chen, P. C.; Kou, K. L. ; Tai, H. K.; Jin, S. L.; Lye, C. L.; Lin, C. Y. (2002). Removal of Carbon Dioxide by Reactive Crystallization in a Scrubber---Kinetics of Barium Carbonate Crystals. *J. Crystal Growth*, *237-239*, pp.2166-2171.

Cournil, M.; Herri, J. M. (2003). Asymptotic Models for Gas-Liquid Crystallization in Two-Film Systems, *AIChE J.*, 49(8), pp.2031-2038.

Danckwerts, P. V. (1970). *Gas-Liquid Reactions*, McGraw-Hill, NewYork, USA.

Degaleesan, S.; Dudukovic, M. P. (1998). Liquid Backing in Bubble Columns and the Axial Dispersion Coefficient, *AIChE J.*, 44(11), pp.2369-2378.

Fan, L. S. (1989). *Gas-Liquid-Solid Fluidization Engineering*; Butterworths: New York, USA.

Hamid, S. N. S.; Jones, A. G. (2002). Scale up of gas-liquid precipitation of calcium carbonate crystals in draft tube bubble columns, *15th Ind. Cry., Serrento, Italy*(2002)(CD-ROM)

Hikita, H.; Asai,S.; Tanigawa, K; Segawa, K; Kitao, M.(1980). Gas hold-up in bubble columns, *The Chemical Engineering Journal*, 20, pp.59-67.

Hudson, J. L.; Rochelle, G. T. (1982). *Flue Gas Desulfurization*, American Chemical Society, ACS Symposium Series 188, Washington, D.C., U.S.A..

Kim, S; Kim, H. T. (2004). Aspen simulation of CO_2 absorption system with various amine solution, *Prepr. Pap.-Am. Chem. Soc., Div. Fuel Chem.*, 49(1), pp.251-252.

Lapin, A.; Paaschen, T.; Junghans, K.; Lubbert, A. (2002). Bubble Column Fluid Dynamics, Flow Structures in Slender Columns with Large-Diameter Ring-Spargers, *Chem. Eng. Sci.*, 57, pp.1419-1424.

Levenspiel, O. (1998). *Chemical Reaction Engineering*, 3rd ed., Chapters 23-24, John Wiley & Sons.

Lin, C. C.; Liu, W. T.; Tan, C. S.(2003). Removal of Carbon Dioxide by Absorption in a Rotating Packed Bed. *Ind. Eng. Chem. Res.*, *42*, pp.2381-2386.

Juvekar, V. A.; Sharma, M.M. Absorption of CO_2 in a suspension of lime, *Chem. Eng. Sci.*, 28, pp.825-837.

Morel, F. M. M. (1983). *Principles of Aquatic Chemistry*; John Wiley & Sons: New York.

Nancollas, G. H.(1966). *Interactions in Electrolyte Solutions*, Elsevier Publishing Company, Amsterdam, Netherlands.

Okawa, T.; Tsuge, H.; Matsue, H. (1999). Reactive crystallization of $CaCO_3$ in a gas-liquid multistage column crystallizer, *14th Ind. Cry.* 1999(CD-ROM)

Sada, E.; Kumazawa, H.; Lee, C.; Fujiwara, N. (1985). Gas-Liquid Mass Transfer Characteristics in a Bubble Column With Suspended Sparingly Soluble Fine Particles, *Ind. Eng. Chem. Process Des. Dev.*, 24, pp.255-261.

Saha, A. K.; Bandyopadhyay, S.S. Absorption of carbon dioxide in alkanolamines in the presence of fine activated carbon particles, *Can. J. Chem. Eng.*, 70, pp.193-196.

Shah, Y. T. (1979). *Gas-Liquid-Solid Reactor Design*; McGraw-Hill; New York.

Sauer, T.; Hempel, D. C. (1987). Fluid dynamics and mass transfer in a bubble column with suspended particles,*Chem. Eng. Technol.* 10, pp.180-189.

Sanchez, O.; Michaud, S.; Escudie, R.; Delgenes, J. P.; Bernet, N.(2005). Liquid Mixing and Gas-liquid Mass Transfer in a Three-phase Inverse Turbulent Bed Reactor. *Chemical Engineering J.*, *114*, pp.114-120.

Shah, Y. T.(1979). *Gas-Liquid-Solid Reactor Design*; McGraw-Hill; New York.

Sherwood, T. K.; Pigford, R. L.; Wilke, C. R. (1975). *Mass Transfer*; McGraw-Hill Inc.; New York.

Sohnel, O.; Garside, J. (1992). *Precipitation*; Butterworth-Heinemann Ltd.: Oxford.

Stewart, C.; Hessami, M. A study of methods of carbon dioxide capture and sequestration---the sustainability of a photosynthetic bioreactor approach, *Energy Conversion and management*, 46, pp.403-420.

Tontiwachwuthikul, P.; Meisen, A.; Lim, J. (1992). CO$_2$ Absorption by NaOH, Monoethanolamine and 2-amino-2-methyl-1-propanol Solutions in a Packed bed, *Chem. Eng. Sci.*, *47*, pp.381-390.

Yang, H.; Xu, Z.; Fan, M; Cupta, R; Slimane, R. B.; Bland, A. E.; Wright, I. (2008). Process in carbon dioxide sepration and capture: A review, *J. of Environmental Sciences*, 20, pp.14-27.

Yeh, A. C.; Bai, H. (1999). Comparison of ammonia and monoethanolamine solvents to reduce CO$_2$ greenhouse gas emissions, *The Science of the Total Environment*, *228*, pp.121-133.

Yeh,J. T.; Resnik, K. P.; Rygle, K.; Pennline, H. W. (2005). Semi-batch absorption and regeneration studies for CO$_2$ capture by aqueous ammonia, *Fuel Processing Technology*, *86*, pp.1533-1546.
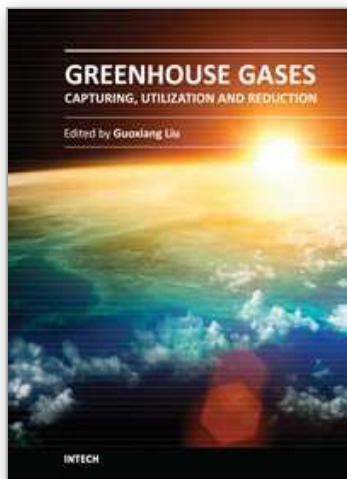
Greenhouse Gases - Capturing, Utilization and Reduction

Edited by Dr Guoxiang Liu

Understanding greenhouse gas capture, utilization, reduction, and storage is essential for solving issues such as global warming and climate change that result from greenhouse gas. Taking advantage of the authors' experience in greenhouse gases, this book discusses an overview of recently developed techniques, methods, and strategies: - Novel techniques and methods on greenhouse gas capture by physical adsorption and separation, chemical structural reconstruction, and biological utilization. - Systemic discussions on greenhouse gas reduction by policy conduction, mitigation strategies, and alternative energy sources. - A comprehensive review of geological storage monitoring technologies.

How to reference

In order to correctly reference this scholarly work, feel free to copy and paste the following:

Pao-Chi Chen (2012). Absorption of Carbon Dioxide in a Bubble-Column Scrubber, Greenhouse Gases - Capturing, Utilization and Reduction, Dr Guoxiang Liu (Ed.), ISBN: 978-953-51-0192-5, InTech, Available from: http://www.intechopen.com/books/greenhouse-gases-capturing-utilization-and-reduction/absorption-of-carbon-dioxide-in-a-bubble-column-scrubber

INTECH
open science | open minds